PRAMANA
— journal of
physics

Vol. 65, No. 5
November 2005
pp. 831–840

On amorphization and nanocomposite formation in Al–Ni–Ti system by mechanical alloying

N DAS[1], G K DEY[2], B S MURTY[3] and S K PABI[1]
[1]Metallurgical and Materials Engineering Department, Indian Institute of Technology, Kharagpur 721 302, India
[2]Bhabha Atomic Research Centre, Mumbai 400 085, India
[3]Metallurgical and Materials Engineering Department, Indian Institute of Technology-Madras, Chennai 600 036, India
E-mail: skpabi@metal.iitkgp.ernet.in

Abstract. Amorphous structure generated by mechanical alloying (MA) is often used as a precursor for generating nanocomposites through controlled devitrification. The amorphous forming composition range of ternary Al–Ni–Ti system was calculated using the extended Miedema's semi-empirical model. Eleven compositions of this system showing a wide range of negative enthalpy of mixing ($-\Delta H^{\mathrm{mix}}$) and amorphization ($-\Delta H^{\mathrm{amor}}$) of the constituent elements were selected for synthesis by MA. The $Al_{88}Ni_6Ti_6$ alloy with relatively small negative ΔH^{mix} (-0.4 kJ/mol) and ΔH^{amor} (-14.8 kJ/mol) became completely amorphous after 120 h of milling, which is possibly the first report of complete amorphization of an Al-based rare earth element free Al–TM–TM system (TM = transition metal) by MA. The alloys of other compositions selected had much more negative ΔH^{mix} and H^{amor}; but they yielded either nanocomposites of partial amorphous and crystalline structure or no amorphous phase at all in the as-milled condition, evidencing a high degree of stability of the intermetallic phases under the MA environment. Hence, the negative ΔH^{mix} and ΔH^{amor} are not so reliable for predicting the amorphization in the present system by MA.

Keywords. Nanocomposite; amorphization; mechanical alloying; Miedema model; Al–Ni–Ti system.

PACS Nos 82.60.Cx; 81.07.Bc; 81.05.Kf; 81.07.Wx

1. Introduction

An attractive method to produce large quantities of nanostructured composites is the controlled devitrification (crystallization) of amorphous solids [1]. In order to generate the amorphous precursor, mechanical alloying (MA) by high-energy ball milling of the elemental powder blends is extensively employed as a 'far from equilibrium' processing route [1,2]. When MA is combined with appropriate consolidation techniques, it should be able to circumvent the limitations of melt spinning with respect to restriction in geometry and size of the resulting nanostructured

multiphase samples. The former has shown potential in the production of the bulk material without microstructure coarsening, which is typical in cast bulk samples [1]. In the early 1990s, Inoue [3] proposed three empirical rules for the achievement of high amorphous forming ability: (i) negative heat of mixing (ΔH^{mix}) among the constituent elements, (ii) significant difference in atomic size ratio, above 12%, among these elements, and (iii) multicomponent alloy systems consisting of more than three elements. Inoue suggested that a highly negative enthalpy of mixing is more conducive for the amorphous phase formation. Recently, due to the increasing interest in the ternary Al–Ni–Ti alloys for structural applications [4–6], this system has been chosen for the present study. Present work attempts to examine, how the enthalpy of mixing (ΔH^{mix}) and amorphization (ΔH^{amor}) correlates with the structures generated by MA in Al–Ni–Ti system. Comprehensive MA investigations of the corresponding binary systems, i.e. Ni–Al, Ni–Ti and Al–Ti [7–12] are available to facilitate the study on MA of the Al–Ni–Ti system. Earlier investigations on MA of the ternary Al–Ni–Ti system [13–16] have mainly focused their attention on either Ti-based or Ni-based compositions, apparently because alloys containing more than 80 at.% Al are difficult to amorphize by MA [17–19].

2. Analytical

Miedema's semi-empirical model [20] for binary systems is a very useful tool to calculate the amorphous forming composition range (AFCR), where ΔH^{mix} is negative. The topic has been extensively reviewed by Weeber and Bakker [21]. The enthalpy of mixing is defined as the difference between the enthalpy of amorphization (ΔH^{amor}) and the enthalpy of solid solution formation (ΔH^{ss}) [22–24]. In the present work, this model has been extended to the ternary system by splitting it to three pseudo-binary systems and neglecting the ternary interaction terms in a manner similar to Bakker *et al* [22], Murty *et al* [23], and Takeuchi and Inoue [25]. Here the mixing enthalpies of the constituent binary sub-systems as a function of their compositions were calculated on the basis of regular solution model [22]. The neglect of the ternary interaction terms due to the non-availability of related data would certainly introduce some unavoidable error in the enthalpy calculations. The AFCR of the Al–Ni–Ti system at room temperature calculated in this manner is displayed in figure 1. The calculated iso-enthalpy contours of ΔH^{amor} for the same system are shown in figure 2. These values of enthalpies in figures 1 and 2 serve as the basis for selection of the alloy compositions for amorphization, to evaluate the role of ΔH^{mix} and ΔH^{amor}.

3. Experimental

The nominal compositions of the eleven alloys studied in the present investigation are superimposed in figures 1 and 2. Elemental blends of these compositions were prepared from high purity (99.5%) Al, Ni and Ti powders of size 15, 15 and 60 μm, respectively.

Mechanical alloying of these blends was carried out in a high energy Fritsch P5 planetary ball mill, in cemented carbide grinding media at a mill speed of 300 r.p.m. and ball to powder ratio 10 : 1, using toluene as the process control agent. The identity and phase evolution at different stages of MA were studied by the X-ray diffraction (XRD) analysis of the milled powders using the Co-K_α radiation ($\lambda = 1.78897$ nm) in a Philip's X'pert PRO high-resolution X-ray diffractometer. Refined values of lattice parameter (a) were calculated from peak positions in the XRD pattern by extrapolation of a against $(\cos^2\theta/\sin\theta)$ to $\cos\theta = 0$ [26]. The average grain size of Al-rich solid solution was determined from the broadening of a Al_{111} reflection after K-α_2 stripping by Philips X'pert Plus software and using Voigt method [27], which allowed judicious elimination of the contribution due to the instrumental and strain effect on the observed peak broadening. For the overlapping peaks, the full width at half intensity maximum and true Bragg angle (2θ) were determined by an appropriate deconvolution exercise. A few samples were examined using JEOL 2000 FX 120 kV transmission electron microscope (TEM).

4. Results

The enthalpies of mixing of the eleven alloys are shown in figure 1. The XRD patterns in figure 3 show the microstructural evolution during milling of alloy 1 ($Al_{30.5}Ni_{37}Ti_{32.5}$), which has the most negative ΔH^{mix} (-24.1 kJ/mol, figure 1) and ΔH^{amor} (-70.6 kJ/mol, figure 2).

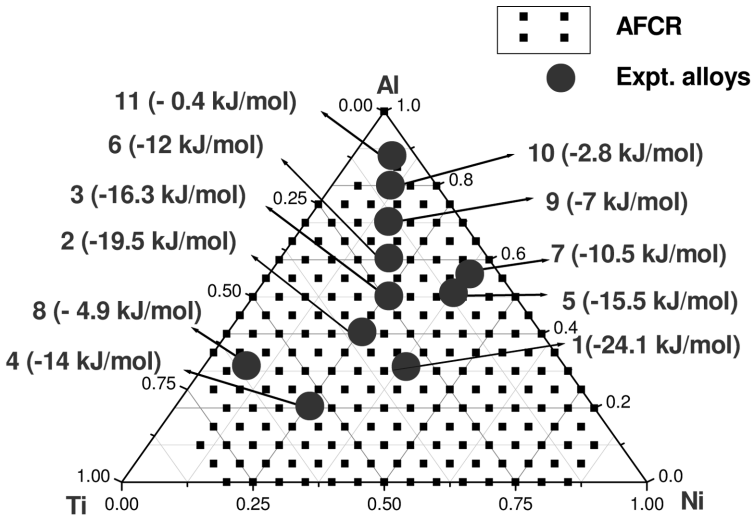

Figure 1. Amorphous forming composition range (AFCR) of the Al–N1–Ti system, predicted by Miedema's model. Composition of the experimental samples are superimposed; here notations like 5 (-15.5 kJ/mol) indicate alloy 5 having $\Delta H^{\text{mix}} = -15.5$ kJ/mol.

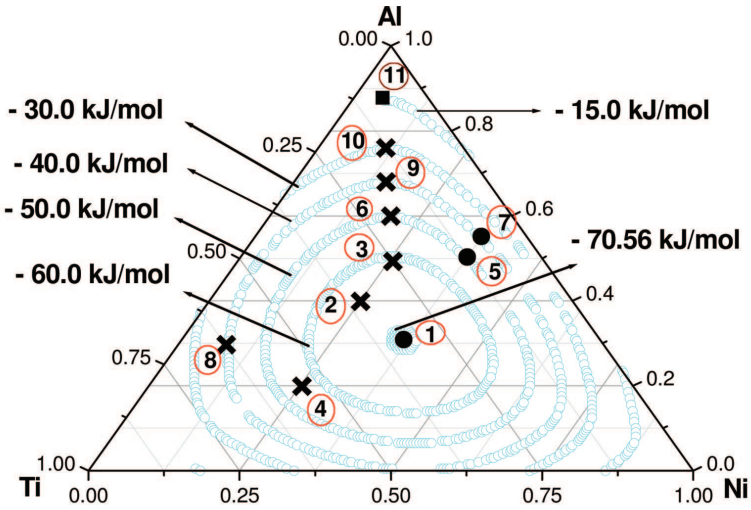

Figure 2. Plots of calculated iso-enthalpy contours of amorphization (ΔH^{amor}). Experimental alloys selected (e.g. 1, 2, etc.) and the phases evolved in them (e.g. amorphous (■), amorphous plus crystalline (✖), and fully crystalline (●)) during MA are also displayed here.

In course of MA of alloy 1 ($Al_{30.5}Ni_{37}Ti_{32.5}$), the $Al_{0.3}Ni_{0.35}Ti_{0.35}$ intermetallic phase appeared after 10 h of MA, and its amount seemed to increase with the progress of milling, as evidenced by the increase in the relative intensities of the corresponding peaks in figure 3. The formation of an amorphous phase was not evident from the XRD patterns at any stage of milling up to 60 h (figure 3). Alloy 5 ($Al_{51}Ni_{37}Ti_{12}$) and alloy 7 ($Al_{55.5}Ni_{37}Ti_{7.5}$) showed similar results during their MA, although they were well inside the AFCR (figure 1).

The alloy 6 ($Al_{60}Ni_{20}Ti_{20}$) was found to form some amorphous phase along with the crystalline phases of AlNi and Ti_3Al after 10 h of milling as is evident from the XRD patterns in figure 4. The TEM micrograph and selected area diffraction (SAD) pattern of alloy 6 at this stage in figure 5 also supported the presence of some amorphous phase along with the crystalline phases. After 20 h of MA the $Al_{0.3}Ni_{0.35}Ti_{0.35}$ intermetallic phase was detectable and the broad maxima corresponding to the amorphous phase became weaker as compared to that after MA for 10 h (figure 4). All the above-mentioned intermetallic phases co-existed in the structure up to 60 h of milling (figure 4) indicating their stability in the MA environment.

Like alloy 6, the MA of alloy 2 ($Al_{40}Ni_{25}Ti_{35}$), alloy 3 ($Al_{50}Ni_{25}Ti_{25}$), alloy 4 ($Al_{20}Ni_{25}Ti_{55}$), alloy 8 ($Al_{31}Ni_8Ti_{61}$), alloy 9 ($Al_{70}Ni_{15}Ti_{15}$) and alloy 10 ($Al_{80}Ni_{10}Ti_{10}$) showed similar trend, i.e. the amorphous plus crystalline phase formed at some intermediate stage of milling, and then on further milling the structure transformed to completely crystalline phase(s). In general, amorphous phase, which forms during non-equilibrium processing (here MA), is a metastable phase, and its further transformation to crystalline phases is possible. Here the presence of the crystalline phase(s) in the amorphous matrix probably provoked this

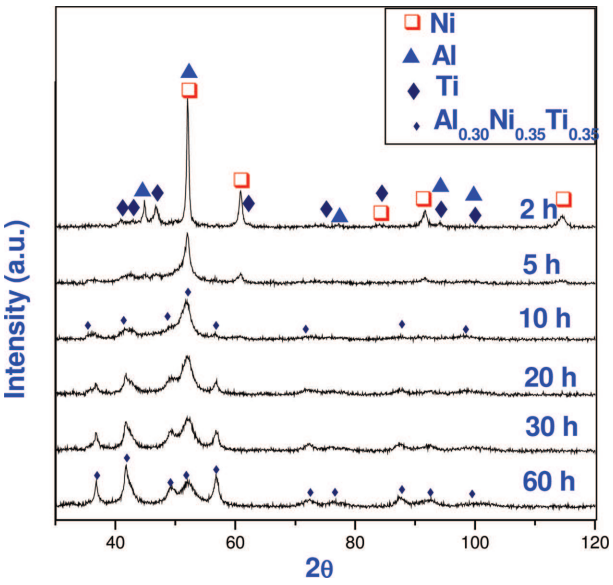

Figure 3. XRD patterns of alloy 1 ($Al_{30.5}Ni_{37}Ti_{32.5}$) show only crystalline phases even after 60 h of MA.

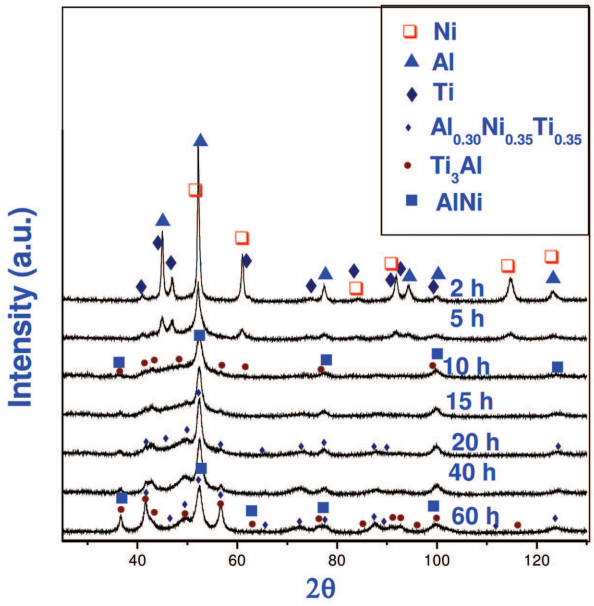

Figure 4. Modulation of XRD patterns of alloy 6 ($Al_{60}Ni_{20}Ti_{20}$) with milling time. After 10 h of milling, crystalline AlNi phase plus amorphous phase formation are evident. With further increase of milling time the structure becomes fully crystalline.

devitrification during further milling. Similar kind of behavior has been reported by Suryanarayana *et al* [28] for Ti–Al alloys (Ti-24 at.% Al and Ti-50 at.% Al), Makifuchi *et al* [29] for Ni–Ti system and Nagarajan *et al* [13] in their study on $Al_{25}Ni_{25}Ti_{50}$ alloy.

Among all the alloy compositions investigated in the present study, alloy 11 ($Al_{88}Ni_6Ti_6$) lying near the periphery of the AFCR in figure 1, and having a very small value of negative enthalpy of mixing ($\Delta H^{\mathrm{mix}} = -0.4$ kJ/mol) and amorphization ($\Delta H^{\mathrm{amor}} = -14.8$ kJ/mol, figure 2) was found to become fully amorphous after 120 h of milling, as evidenced by a broad maxima in the XRD pattern (figure 6) and a diffused ring in the SAD pattern in figure 7 recorded in the TEM.

An insight into the amorphous phase formation in the alloy 11 during MA can be obtained from the variation of lattice parameter (a_{Al}) and crystallite size of Al with milling time in the alloy 11 (figure 8). Here in the early stages of MA from 2 to 5 h, the intensity of Ni peak markedly diminished (figure 6) with concurrent reduction in a_{Al} (figure 8), which apparently indicated a significant extent of dissolution of Ni in Al after nanocrystallization of Al matrix, because the atomic diameter of Ni (0.249 nm) is smaller than that of Al (0.286 nm). In fact, computer simulation by Pabi *et al* [30] has earlier shown that nanostructure formation in the MA process is a prerequisite of any significant rate of alloying. When the milling was extended beyond 5 h, a_{Al} decreased (figure 8) and relative intensity of the Ti peaks diminished (figure 6) up to 30 h of MA, which may be attributed to the dissolution of the larger sized Ti atoms (dia. 0.289 nm) in the Al-rich matrix. The a_{Al} practically remained unchanged beyond 30 h of MA (figure 8) apparently indicating the completion of dissolution of Ni and Ti in the Al matrix. Figure 6 also evidences the presence of some amorphous phase after 30 h of milling. Further milling continued to refine the crystallite size of Al (figure 8), and ultimately destabilized the crystalline structure presumably by the accumulation of mechanical disorder in the Al solid solution to yield a completely amorphous structure after 120 h of milling (figure 6).

5. Discussion

Inoue [31] classified the amorphous forming alloys into five groups, namely: (i) ETM–Al–LTM, (ii) LTM–Al–B (or Si), (iii) LTM–ETM–METTALLOID, (iv) LTM–METALLOID, (v) Mg–Ln–LTM and ETM (Zr, Ti)–Be–LTM (LTM: late transition metal and ETM: early transition metal). It is known that complete amorphization is very difficult to achieve during MA of the alloys containing more than 80 at.% Al, and often the structure shows coexistence of an amorphous phase and fcc Al-rich matrix with some intermetallic compound(s) [17–19]. Schurack *et al* [32,33] reported for the first time complete amorphization in such an Al-based alloy ($Al_{85}Y_8Ni_5Co_2$) with rare-earth element Y [34] by systematic variation and optimization of the milling parameters. To the best of our knowledge, amorphization of $Al_{88}Ni_6Ti_6$ composition is possibly the first report of complete amorphization of a ternary Al-rich (>80 at.%) Al–ETM–LTM system by MA.

In the present system it was found that amorphous plus some crystalline phases or only crystalline phases formed during MA of the alloys 1–10, which had more negative values of ΔH^{mix} and ΔH^{amor} (figures 1 and 2). It is known that the enthalpy of

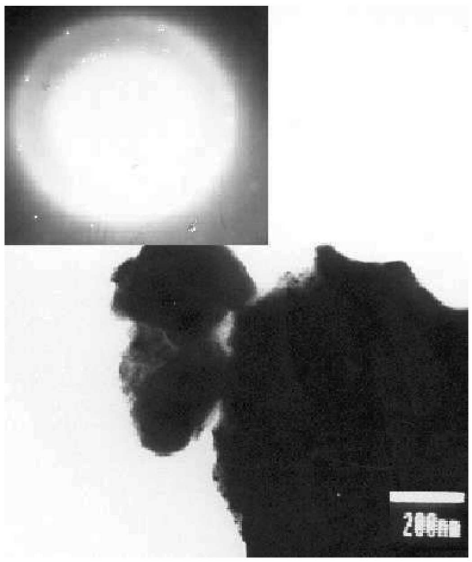

Figure 5. Transmission electron micrograph of alloy 6 ($Al_{60}Ni_{20}Ti_{20}$) after 10 h of MA. The SAD pattern in the inset shows diffuse ring from amorphous phase and few sharp spots from crystalline phase.

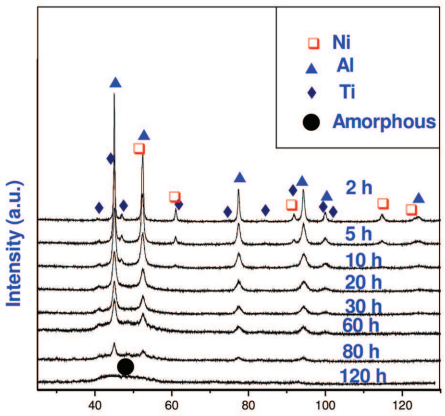

Figure 6. XRD patterns of alloy 11 ($Al_{88}Ni_6Ti_6$) evidencing the presence of amorphous phase only after MA for 120 h.

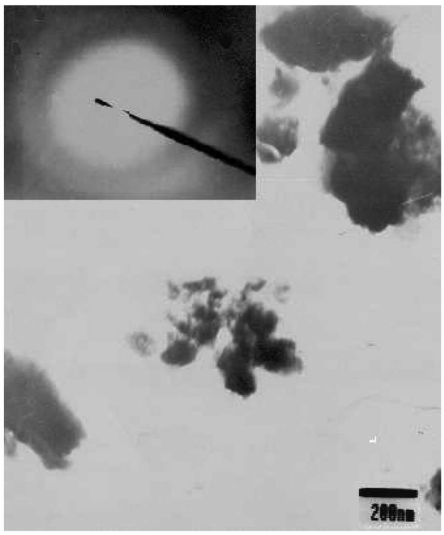

Figure 7. Transmission electron micrograph of alloy 11 ($Al_{88}Ni_6Ti_6$) after 120 h of MA. The SAD pattern in the inset shows only a diffused ring.

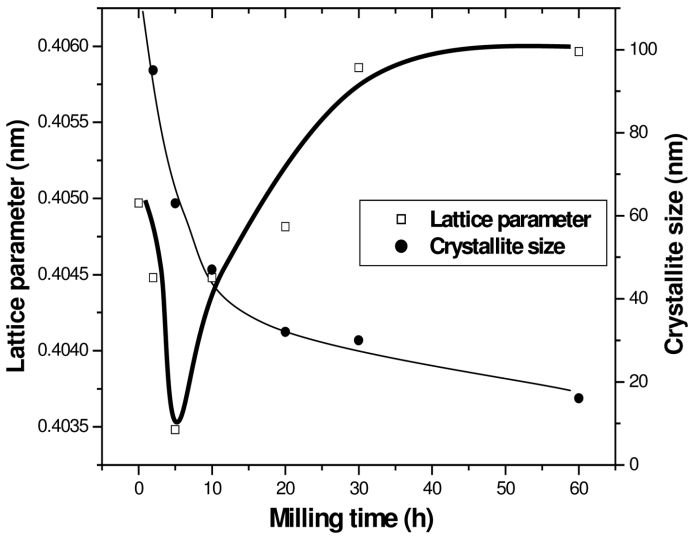

Figure 8. The variation of crystallite size and lattice parameter of Al during the milling of alloy 11 ($Al_{88}Ni_6Ti_6$).

formation of intermetallic compounds is usually much more negative than that for the corresponding amorphous phase formation [20]. But the Miedema's model cannot predict the compositions at which such intermetallic phases would form in any given system. In case of MA, the chances of formation of any intermetallic phase(s) utilizing only a part of the constituents and/or the phase evolution sequence can be quite different from that in rapid solidification processing (RSP), and this can explain, why the experimentally observed glass-forming compositions in RSP are often different from that for MA [17–19]. These factors coupled with the simplifications inherent in the present model (see §2) might have led to the prediction of a wider AFCR compared to that of the experimentally observed model.

In summary, the absolute values of ΔH^{amor} and ΔH^{mix} do not seem to be the appropriate criteria for amorphization in the Al–Ni–Ti system. The kinetic factors like the competition between the amorphization and crystallization, and the structural factors like the extent of the crystallite size refinement and the stability of any intermetallic phase(s) formed during milling under continued deformation may have a decisive role in the amorphization by MA.

6. Conclusions

Complete amorphization by mechanical alloying (MA) could be achieved for the first time in a ternary Al-rich (i.e. >80 at.% Al) Al–ETM–LTM alloy, namely, $Al_{88}Ni_6Ti_6$. Here the dissolution of Ni and Ti in the Al matrix, coupled with the structural defects induced by the MA process seemed to promote amorphization. In contrast, nanocomposites of amorphous plus crystalline phases formed at intermediate stages of MA in compositions like $Al_{40}Ni_{25}Ti_{35}$, $Al_{50}Ni_{25}Ti_{25}$, $Al_{20}Ni_{25}Ti_{55}$,

$Al_{60}Ni_{20}Ti_{20}$, $Al_{31}Ni_8Ti_{61}$, $Al_{70}Ni_{15}Ti_{15}$ and $Al_{80}Ni_{10}Ti_{10}$; but they became fully crystalline on further milling apparently due to the stability of these intermetallic phases under milling condition. The magnitude of the negative enthalpies of mixing (ΔH^{mix}) and amorphization (ΔH^{amor}) are not reliable for predicting the amorphization in the Al–Ni–Ti system in course of MA.

Acknowledgements

This work is sponsored by the Department of Science and Technology grant No. SR/S5/NM-S1/2002. One of the authors (ND) acknowledges the financial support of the Department of Atomic Energy, Govt. of India vide grant No. PD/8(5)/02/R-IV/DGFS/697.

References

[1] J Eckert, in *Nanostructured merials – Processing, properties and potential applications* edited by C C Koch (Noyes, New York, 2002) p. 432
[2] C Suryanarayana, *Int. Mater. Rev.* **40**, 41 (1995)
[3] A Inoue, *Bulk amorphous alloys – Preparation and fundamental characteristics*, Materials Science Foundation (Trans Tech, The Netherlands, 1998) Vol. 4, p. 1
[4] K S Kumer, *Int. Mater. Rev.* **35**, 293 (1990)
[5] S Naka, M Thomas and T Khan, *Mater. Sci. Tech.* **8**, 291 (1992)
[6] R Yang, J A Leake and R W Cahn, *J. Mater. Res.* **6**, 343 (1991)
[7] E Ivanov, T Gregorieva, G Golubkova, V Boldyran, A B Fasman, S D Mikhailenko and O T Kalinina, *Mater. Lett.* **7**, 51 (1988)
[8] M Atzmon, *Phys. Rev. Lett.* **64**, 487 (1990)
[9] R B Schwarz, R R Petrich and C K Saw, *J. Non-Crvst. Solids* **76**, 281 (1985)
[10] T Itzukaichi, S Ohara, J G Cabanas-Moreno, M Umemoto and I Okane, *J. Mater. Sci.* **29**, 1481 (1994)
[11] W Guo, S Martelli, N Burgio, M Magini, F Padella, E Paradisco and I Soletta, *J. Mater. Sci.* **24**, 6190 (1991)
[12] C Suryanarayana, G H Chan, A Frefer and F H Froes, *Mater. Sci. Eng.* **A158**, 93 (1992)
[13] R Nagarajan and S Ranganathan, *Mater. Sci. Eng.* **A179/A180**, 168 (1994)
[14] T Itzukaichi, M Umemoto and J G Cabanas-Moreno, *Scripta. Metall. Mater.* **29**, 583 (1993)
[15] M Umemoto, T Itzukaichi, J Cabanas-Moreno and I Okane, in *Mechanical alloying for structural applications* edited by J J de Barbadillo, F H Froes and R Schwarz (1993) p. 245
[16] Z G Liu, J T Guo and Z Q Hu, *Mater. Sci. Eng.* **A192/A193**, 577 (1995)
[17] T Benameur, A Inoue and T Masumoto, *Mater. Trans. JIM* **35**, 451 (1994)
[18] T Benameur, A Inoue and T Masumoto, *Nanostruct. Mater.* **4**, 303 (1994)
[19] M Seidel, J Eckert, H D Bauer and L Schultz, in *Grain size and mechanical properties – Fundamentals and applications* edited by M A Otooni, R W Armstrong, N J Grant and K Ishizaki (*Mater. Res. Soc. Symp. Proc.*, Materials Research Society, Warrendale, PA, 1995) Vol. 362, p. 239

[20] F R Boer and D G Perrifor, *Cohesion in metals* (Elsevier, The Netherlands, 1998) p. 1
[21] A W Weeber and H Bakker, *Physica* **B153**, 93 (1988)
[22] H Bakker, G F Zhow and H Yang, *Prog. Mater. Sci.* **39**, 241 (1995)
[23] B S Murty, S Ranganathan and M M Rao, *Mater. Sci. Eng.* **A16**, 231 (1992)
[24] H Bakker, in *Enthalpies in alloys* (Trans Tech, The Netherlands, 1998) p. 1
[25] A Takeuchi and A Inoue, *Mater. Trans.* **42**, 1435 (2000)
[26] B D Cullity, *Elements of X-ray diffraction*, 2nd Edition (Addison Wesley, Reading, MA, 1978) p. 350
[27] T H Keijser, I L Langford, E J Mittemeijer and B P Nogel, *J. Appl. Cryst.* **15**, 314 (1982)
[28] C Suryanarayana, G H Chen and A Frefer, *Mater. Sci. Eng.* **A158**, 93 (1992)
[29] Y Makifuchi, Y Terunuma and M Nagumo, *Mater. Sci. Eng.* **A226–228,** 312 (1997)
[30] S K Pabi, D Das, T K Mahapatra and I Manna, *Acta Mater.* **46**, 3501 (1998)
[31] A Inoue, *Acta Mater.* **48,** 279 (2000)
[32] F Schurack, I Borner, J Eckert and L Schultz, in *Metastable, mechanically alloyed and nanocrystalline materials* edited by A Calka and D Wexler (Trans. Tech, Zurich, 1999) p. 312.
[33] F Schurack, I Borner, J Eckert and L Schultz, *J. Metastable and Nanocrystalline Mater.* **49**, 2 (1999)
[34] A Cotton, G Wilkinson, C A Murillo and M Bochman, in *Advanced inorganic chemistry* (John Willey, New York, 1999) p. 1108